Vibrational Spectroscopy 64 (2013) 148–152

Contents lists available at SciVerse ScienceDirect

Vibrational Spectroscopy

journal homepage: www.elsevier.com/locate/vibspec

Short communication

# Raman and infrared spectra of brookite ($TiO_2$): Experiment and theory

M.N. Iliev*, V.G. Hadjiev, A.P. Litvinchuk

*Texas Center for Superconductivity, University of Houston, Houston, TX 77204-5002, USA*

ARTICLE INFO

*Article history:*
Received 17 June 2012
Received in revised form 1 August 2012
Accepted 2 August 2012
Available online 13 August 2012

*Keywords:*
Raman spectroscopy
Infrared spectroscopy
Brookite
$TiO_2$
Phonons

ABSTRACT

The zone-center phonons and the frequency-dependent dielectric function of the brookite phase of $TiO_2$ are studied experimentally by means of polarized Raman and infrared spectroscopy. The Raman- and infrared-active modes are unambiguously identified by symmetry. The mode frequencies are in good agreement with those predicted by the density function calculations of lattice dynamics.

## 1. Introduction

The brookite form of $TiO_2$ [SG#61, $D_{2h}^{15}(Pbca)$, $Z = 8$, see Fig. 1] is less studied than the more common rutile [SG#136, $D_{4h}^{14}(P42/mnm)$, $Z = 2$] and anatase [SG#141, $D_{4h}^{19}(I41/amd)$, $Z = 4$] $TiO_2$ polymorphs. Such studies have been partly hampered by the difficulty to synthesize pure brookite unaccompanied by anatase and/or rutile phases. In the past few years, however, there is an increased interest to this polymorph as both, methods of preparation of pure brookite have been developed [1–4] and a high potential for application has been revealed [4,5].

Raman spectroscopy has been widely used to detect the presence of the brookite phase in $TiO_2$ containing materials, usually in close comparison with the Raman spectra of natural brookite crystals reported by Tompsett et al. [6]. The lower symmetry and larger unit cell of brookite result in a larger number of Raman and infrared-active phonons compared to anatase and rutile structures. From symmetry considerations one expects 36 $(9A_{1g} + 9B_{1g} + 9B_{2g} + 9B_{3g})$ Raman active, 24 $(8B_{1u} + 8B_{2u} + 8B_{3u})$ infrared active modes, as well as $9A_{1u}$ silent and three $(B_{1u} + B_{2u} + B_{3u})$ acoustic modes. In the study of Tompsett et al. [6] in total 25 Raman lines have been observed and assigned to modes of definite symmetry. Some of these assignments, however, will be challenged in this work. There are few reports on the infrared spectra of brookite in the phonon energy range. Interestingly, the most reliable data so far came from the astrophysical community. In the work of Posch et al. [7] an oscillator fit of polarized reflectance spectra combined with Kramers–Kronig analysis have been used to derive the optical constants. These constants have further been used to calculate the effective absorption (and scattering) cross sections of arbitrarily oriented brookite particles which are part of the circumstellar dust. Unfortunately, the positions of the maxima in the polarized absorption spectra that could be used to determine and distinguish the $B_{1u}$(TO), $B_{2u}$ (TO), and $B_{2u}$(TO) phonon wavenumbers are not directly given.

In addition to the experimental studies, the lattice dynamics and electronic structure of brookite has also been studied theoretically in the framework of density functional theory (DFT) [8]. While there is an adequate correspondence between the experimental and theoretical Raman $A_{1g}$ frequencies, no comparison has been possible for the infrared-active phonons and corresponding LO–TO splittings as no sufficient experimental data have been available.

In an attempt to firmly verify the phonon structure of brookite and complete the assignment of the $\Gamma$-point phonon modes, we measured the polarized Raman spectra of brookite in several exact scattering configurations using different excitation laser lines. The assignments of part of the lines were confirmed, whereas the rest lines were either previously reported but now reassigned to modes of different symmetry, or newly observed and identified.

We also measured the infrared reflectance spectra between 50 and 3000 $cm^{-1}$ with light polarized along the crystallographic axes, which allowed us through Kramers–Kronig analysis to derive the optical constants, conductivity and loss function, thus making possible to identify experimentally the TO and LO components of the infrared active modes.

---

* Corresponding author. Tel.: +1 713 743 8209; fax: +1 713 743 8201.
*E-mail address:* miliev@uh.edu (M.N. Iliev).

0924-2031/$ – see front matter © 2012 Elsevier B.V. All rights reserved.
http://dx.doi.org/10.1016/j.vibspec.2012.08.003

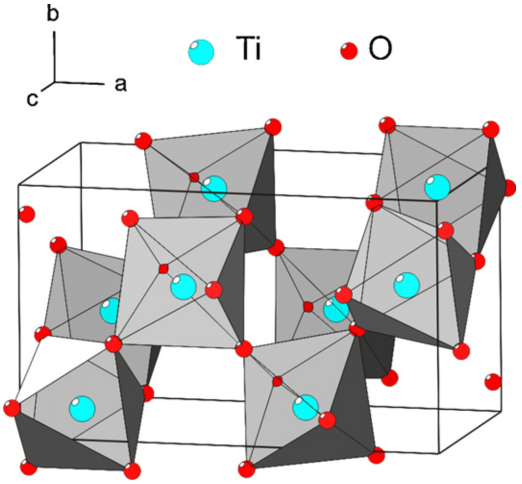

**Fig. 1.** Elementary cell of brookite.

To complete the study of the lattice dynamics of brookite, the experimentally observed phonon frequencies are compared to those predicted by DFT calculations.

## 2. Material and methods

The samples used in these experiments were natural brookite crystals from Magnet Cove, Arkansas (Fig. 2) similar to those described in [9]. The Raman spectra were collected at room temperature under microscope from (1 0 0), (1 0 0), and (0 0 1) surfaces using 633 nm (1.96 eV), 515 nm (2.41 eV), or 458 nm (2.71 eV) excitation. The symmetry of the Raman lines can readily be identified by their presence or absence in spectra obtained in exact scattering configurations. The $A_{1g}$ modes are allowed with parallel *XX*, *YY*, or *ZZ* scattering configurations and forbidden with crossed *XY*, *XZ*, and *YZ* configurations. In these notations the first and second letters stay, respectively, for the polarization of the incident and scattered light, $X \parallel [1\,0\,0]$, $Y \parallel [0\,1\,0]$, $Z \parallel [0\,0\,1]$. The allowed configurations for the $B_{1g}$, $B_{2g}$, and $B_{3g}$ modes are *XY*, *XZ*, and *YZ*, respectively.

The reflection measurements in polarized light were performed on a Bomem-DA8 Fourier-transform interferometer in the range 50–5000 cm$^{-1}$ with the use of a liquid–helium-cooled bolometer and a liquid-nitrogen cooled HgCdTe detector, as well as appropriate beam splitters. Spectral resolution was set to 1 cm$^{-1}$. Below the lowest measured experimental frequency the reflectance spectra $R(\omega)$ were extrapolated by a constant, which is a standard procedure for treating insulating samples. The Kramers–Kronig analysis was further performed in order to obtain the real and imaginary parts of the dielectric function and other related optical functions.

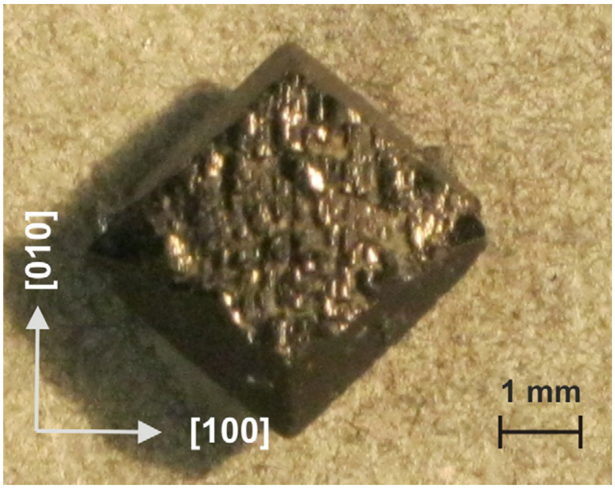

**Fig. 2.** Brookite crystal.

## 3. DFT calculation details

The DFT calculations were done within the generalized-gradient approximation (GGA) with Perdew–Burke–Ernzerhof (PBE) exchange-correlation functional [10] using the norm-conserved pseudopotential plane-wave method as implemented in the CASTEP code [11]. The electronic band structure, related properties, and geometry optimization of the structures were calculated self-consistently (SCF) with 830 eV kinetic energy cutoff for the plane waves and SFC tolerance better than $5 \times 10^{-7}$ eV/atom over $2 \times 3 \times 3$ Monkhorst–Pack grid in the k-space. The band structure calculations of brookite revealed a non-metallic system and fixed electron occupancy constrains were imposed on the SCF energy minimization as a prerequisite for using the linear response DFT code [12] in the phonon calculations.

Brookite ($TiO_2$) crystallizes in an orthorhombic structure with lattice parameters $a = 9.184$ Å, $b = 5.447$ Å, and $c = 5.145$ Å measured by X-ray diffraction [13]. We preserved the value of the experimental lattice parameters during optimization of the structure through relaxing only the in-cell atomic positions within the BFGS minimization scheme [14]. During minimization the maximum deviation from crystal symmetry was constrained to $1.01 \times 10^{-15}$ Å until completed with convergence parameters $3.5 \times 10^{-6}$ eV/atom for energy, $6.0 \times 10^{-3}$ eV/Å for forces, 0.02 GPa for stresses, and $5 \times 10^{-4}$ Å for displacements. The optimization of the brookite crystal structure with relaxed both lattice parameters and atomic positions resulted in a structure with $a = 9.203$ Å, $b = 5.473$ Å, and $c = 5.150$ Å. In this case the total energy of the systems lowers by only $10^{-5}$% with respect to that of the structure with fixed experimental lattice parameters. However, we report here only the calculated phonon frequencies for the optimized structure with experimental lattice parameters because they are closer to experimental ones than those of the fully relaxed structure. The phonon wavenumbers of brookite were calculated by using the linear response DFT scheme [12] in which the atomic displacements are treated as perturbation. The response of the brookite model system to electric field was calculated in order to make a non-analytical correction to the dynamic matrix elements at the Γ-point and thus to calculate the LO phonon wavenumbers.

## 4. Results and discussion

### 4.1. Raman spectra

Fig. 3 shows the Raman spectra of brookite in parallel *XX*, *YY*, and *ZZ* configurations, where only the $A_{1g}$ modes are allowed. In addition to the seven $A_{1g}$ modes reported by Tompsett et al. [6] (at 125, 152, 194, 246, 412, 492, and 640 cm$^{-1}$), the two missing modes of this symmetry are also clearly observed at 324 and 545 cm$^{-1}$. The relative intensity of the Raman lines exhibits only modest variation with excitation photon energy. The $A_{1g}$ wavenumbers obtained by DFT calculations (shown at the bottom of Fig. 3) are in a very good agreement with the experimental values. The atomic motions corresponding to the $A_{1g}$ modes are illustrated in Fig. 4. The experimental and theoretical data on the Raman phonons of brookite are summarized in Table 1. The eigenvectors for all Γ-point phonon modes, as obtained from the DFT calculations are given in Supplementary data.

The *XY* ($B_{1g}$), *XZ* ($B_{2g}$), and *YZ* ($B_{3g}$) spectra are shown in Fig. 5 along with the DFT calculated values. The $B_{2g}$ Raman line